Supplementary Information for

Complex contagion process in spreading of online innovation

M. Karsai*, G. Iñiguez, K. Kaski, J. Kertész

*Corresponding author email: marton.karsai@ens-lyon.fr

Contents

S1 Data description

This research is based on a dataset with a temporally detailed description of the social network of (anonymized) Skype users. It covers the history of users adopting Skype from September 2003 until March 2011 (2738 days), including registration events and contact network evolution for every registered users in Skype [1] all around the world. For each user, the dataset provides the following details:

- Date and country of registration.
- Time-stamped events of link additions.

In the Skype network, when a user adds a friend to the contact list, the friend may confirm the contact invitation or not. Thus, links are added by means of the following events: contact addition and contact confirmation. In our study we capture trusted social links by retaining confirmed edges only, i.e. edges where both parties have acknowledged the connection. Failure to do so would lead to a mix of undesired and desired connections.

For our investigations we select user accounts with identified countries of registration and consider all confirmed connections between users. To receive the best estimation of node degrees in the underlying social network, we integrate the evolving Skype network for the whole available period and count the number of confirmed relationships per node, including international ties as well.

The adoption dynamics of a given country may be directly observed by assigning times of adoption (t_a) and termination (t_t) for all accounts. They are respectively defined as the dates of registration and last activity in Skype. Explicitly, we identify an account as terminated if its last activity happened earlier than one year prior to the end of the observation period. In this way we built the complete adoption and termination history of the Skype product for 2373 days.

S2 Empirical measures of spreading parameters

As discussed in the main text, we are able to estimate some of the model parameters directly from the empirical data. In what follows we describe in detail the definitions and limitations of the measurements for p_a, p_p, $p(n)$ and p^-, and shortly discuss the matching of the time scales of the real and model dynamics.

S2.1 Average number of social ties

Online social networks have the common limitation that, even while uncovering several characteristics of the real social graph underneath, they can only map a subset of the existing social relationships. This is simply because not everyone is registered to a given online service and thus not all social contacts are recorded. However, one may make the assumption that the online network, although only a sample of the real social graph, serves as a good proxy for the structure of society. This approximation is more reliable in technologically-advanced countries where the usage of online social services and communications is high, since the online sample is more representative.

We follow this line of thought and aggregate the evolving online social network of Skype between users of the same country for the whole available 7.5 years. In this way we receive a static aggregated structure as the best approximation of the actual social structure. Then we consider all international connections linking country users to accounts in any other nation, and finally estimate $\widetilde{\langle k \rangle}$ as the average number of friends of a given individual, or ego. The observed ego networks are still incomplete, meaning that the estimated degree is bounded by its real value of the underlying social network, $\widetilde{\langle k \rangle} \leq \langle k \rangle$. Even though this estimation process induces certain bias in the measurement (further discussed in section S2.3), its precision increases with larger values of $\widetilde{\langle k \rangle}$.

[1] At the end of 2010 Skype had more than 663 million registered accounts, as reported in [1].

S2.2 Probability of spontaneous adoption

The probability of spontaneous adoption p_a can be estimated directly from the data without any bias. The only things we need to know is when someone registered to Skype and whether such user was the first to adopt among his/her friends, independently of the degree of the user. Thus the probability of spontaneous adoption per unit time can be measured as,

$$p_a(t) = \frac{\#ad(t + \Delta t | SF = 0)}{I - N_a(t)}, \tag{S1}$$

where $\#ad(t+\Delta t|SF = 0)$ is the number of users who adopted Skype during the period $[t, t+\Delta t]$, under the condition that none of their (later emerging) neighbors adopted before them. At each time step, this count is normalized by the total number of people who are not using Skype, i.e. the difference between the number of internet users I in a given country and the number of users at time t, $N_a(t)$. By looking at the time evolution of $p_a(t)$ (orange curve in Fig. 2B, main text), it is clear that after an initial transient period this probability saturates and fluctuates around a constant value $\widetilde{p_a}$. Such value is the estimated average probability of spontaneous adoption in the interval Δt, which may then be used for the model calculations.

Even if the obtained rate approaches a constant for some countries, the observation time in the dataset is not sufficient to get the empirical estimate $\widetilde{p_a}$ in all cases. For consistency in our study, then, we leave p_a as a free model parameter to be fitted. From the 34 countries studied, only 11 show a sufficiently fast adoption process such that $p_a(t)$ reaches a stationary value. A list of these countries is shown in Table S1, and the matter of an empirically vs. freely determined p_a parameter is discussed in section S4.

S2.3 Probability of peer-pressure adoption

Unfortunately, we cannot follow the same strategy in order to estimate the probability for peer-pressure adoption p_p. One could calculate a quantity analogous to that of Eq. (S1),

$$p_p(t) = \frac{\#ad(t + \Delta t | SF \neq 0)}{I - N_a(t)}, \tag{S2}$$

where $\#ad(t + \Delta t|SF \neq 0)$ is the number of adoption events per unit time, such that each adopting individual has at least one (or more) user neighbors at the moment of adoption. However, this quantity depends on the degree (k_i) and number of user friends (N_i) of any adopter i, and is thus driven by strong nonlinear network effects and node heterogeneity. This nonlinear behavior is evidenced by the time evolution of $p_p(t)$ (brown line in Fig. 2B, main text), where the calculated probability increases in time instead of saturating to a constant.

A more appropriate way to quantify the effect of peer-pressure starts by measuring $n_i = N_i/k_i$, the fraction of user friends of each node i at the time of adoption. However, in the integrated Skype graph we can only measure an effective degree $\widetilde{k_i}$ ($\leq k_i$) and thus an effective fraction $\widetilde{n_i} = N_i/\widetilde{k_i}$ ($\geq n_i$). Even as an approximation, this quantity can still show the qualitative effect of peer pressure in the likelihood of adoption.

With the value of $\widetilde{n_i}$ for all nodes in the integrated network, we can calculate the average conditional probability that a user adopts Skype given that an effective fraction $\widetilde{n}$ of his/her neighbours has already joined the network,

$$p(\widetilde{n}) = \frac{\#ad(\widetilde{n})}{N - \sum_{m=0}^{m<\widetilde{n}} \#ad(m)}, \tag{S3}$$

where the numerator is the number of users with a fraction $\widetilde{n}$ of Skype friends at the time of adoption. The denominator is the number of people with a larger or equal fraction $m \geq \widetilde{n}$, i.e. all individuals who had the chance to adopt Skype while having a fraction $\widetilde{n}$ of user neighbours. This count must exclude those people who have already adopted Skype due to weaker social pressure. Since we cannot

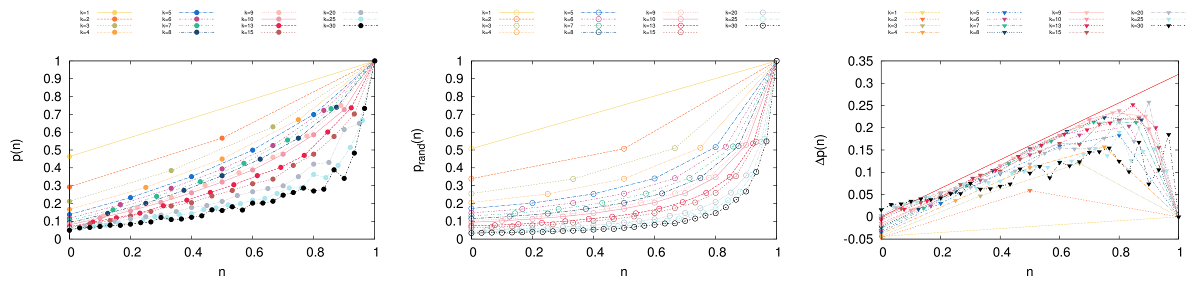

A **B** **C**

Figure S1. Probability of adoption driven by social influence. Conditional probability of adoption as a function of the effective fraction $\widetilde{n}$ of user neighbors. Panel (A) depicts $p(\widetilde{n}, \widetilde{k})$, the conditional probability for nodes of given effective degree $\widetilde{k}$, while panel (B) shows the similar measure $p_{\text{rand}}(\widetilde{n})$ coming from a random reference system where the times of adoptions are shuffled. Panel (C) depicts the difference $\Delta p(\widetilde{n}, \widetilde{k}) = p(\widetilde{n}, \widetilde{k}) - p_{\text{rand}}(\widetilde{n}, \widetilde{k})$ calculated for each degree.

see the entire social network (only the part uncovered by the Skype graph), this probability must take the extreme value $p(\widetilde{n}) = 1$ at $\widetilde{n} = 1$ and is thus increasingly biased as $\widetilde{n} \to 1$. To see the real effect of peer pressure on the probability of adoption $p(\widetilde{n})$, we need to remove the effect of this bias. To this end, we define a random reference model where the termination time is set to infinity and shuffle the adoption times of all accounts. This null model is similarly biased by the effective quantities, but does not include the effects of social influence. Additionally, the null model conserves the adoption rates and keeps the social structure unchanged. In consequence, the empirical and null model values of the probability $p(\widetilde{n})$ differ only in the presence or absence of social influence, and thus their difference should quantify correctly the strength of social pressure and its effect on the probability of service adoption.

In Fig. S1A we show $p(\widetilde{n}, \widetilde{k})$, the conditional probability of adoption for nodes with given effective degree $\widetilde{k}$. Since $\widetilde{n}$ depends on $\widetilde{k}$ this probability takes discrete values, which is apparent for very small degrees. Similar effects can be observed in Fig. S1B, where the corresponding curves $p_{\text{rand}}(\widetilde{n}, \widetilde{k})$ for the null model are shown for nodes of different degrees. The difference $\Delta p(\widetilde{n}, \widetilde{k}) = p(\widetilde{n}, \widetilde{k}) - p_{\text{rand}}(\widetilde{n}, \widetilde{k})$ in Fig. S1C shows that the effect of peer pressure increases linearly with the fraction of adopter neighbours, a rather robust behaviour in terms of degree. The slope of the linear regime may give an estimate $\widetilde{p_p}$ for the value of the probability of peer pressure adoption; however since we only use effective degrees in this calculation, the estimate is actually an upper limit for the real value, $p_p \leq \widetilde{p_p}$. The linear scaling breaks down around $\widetilde{n} \sim 0.8$, a value after which the peer pressure effect decreases radically. Several hypothesis can be introduced to explain this behaviour based on the individualist behaviour of an ego or on his or her reluctance to accept novel technologies, but these discussions are beyond the scope of the present study.

S2.4 Probability of termination

As discussed in the main text, in our model the agents may terminate Skype usage in two different ways: either temporarily and going back into state S, or permanently going into state R, each with respective probability p_s and p_r. In the former case agents may eventually readopt and enter state A again, while in the latter they are removed and stay in state R till the end of the process. Based on the empirical information provided by our dataset, we are not able to directly differentiate between temporary and permanent termination (since Skype accounts are not tied to uniquely identified individuals, who might or might not have multiple accounts) and thus measure the two probabilities independently. Instead we may measure the probability of overall termination,

$$p^{-}(t) = \frac{\#tr(t + \Delta t)}{N_a(t)}, \tag{S4}$$

where $\#tr(t+\Delta t)$ is the number of terminating users in the interval $[t, t+\Delta t]$, out of $N_a(t)$ possible users. Similarly to $p_a(t)$, the probability $p^-(t)$ is not biased by the incomplete social structure, and reaches a constant value $\widetilde{p^-}$ after an initial transient period (blue line in Fig. 2D, main text). This behaviour also holds for the decoupled probabilities of spontaneous and peer-pressure termination,

$$p_a^-(t) = \frac{\#tr(t+\Delta t, TF=0)}{N_a(t)} \quad \text{and} \quad p_p^-(t) = \frac{\#tr(t+\Delta t, TF\neq 0)}{N_a(t)}, \tag{S5}$$

where TF is the number of terminated friends of the ego at the time of his/her own termination. Unlike in the case of adoption, both of these probabilities evolve towards a steady state, suggesting that termination is not driven by non-linear mechanisms and can be characterized by a constant rate. Note that by measuring $\widetilde{p^-}$ and using its definition in the model (see Eq.S8), we may estimate the parameter p_s (or equivalently p_r) with the value,

$$\widetilde{p_s} = \frac{\widetilde{p^-} - p_r}{1-p_r}. \tag{S6}$$

Consequently, a steady termination process allows us to reduce the number of free parameters in the model by one.

S2.5 Time scales

In order to match the time scales of the empirical and modelled rate sequences (seen in Fig. 2A of the main text), we let the time unit of the real process unchanged but introduce a constant $q = N_{int}/N_{pop}$ to rescale the model time as $t' = qt$. Here N_{int} and N_{pop} are the number of internet users and the population of a given country, respectively. Their ratio captures the average societal impact due to a digitally enabled sub-population that modulates the adoption of online products. Since we only rescale the model time while keeping the empirical sequences unchanged, this rescaling does not affect the time scale of the real adoption curves. As a result, the fits and model predictions are obtained in real time as well, independently of q. However, note that in order to correctly estimate model parameters from the data, we need to rescale their values as $p'_*(t') = qp_*(t)$ (where p_* denotes either p_a or p^-).

S3 Model

To simulate and predict the evolution of Skype adoption, we first need to synthesize the observed mechanisms into simple probabilistic rules, and then integrate them into a process modelling the interactions of a large number of individuals. We assume the existence of an underlying social network with arbitrary correlations and slow temporal evolution, in which individuals may choose to become users of the Skype product and give rise to an evolving account network. Our aim is to describe the temporal evolution of the account network with a suitable agent-based model. Under this approach we assume that individuals may start using Skype either by

(a) adopting the product spontaneously, or by

(b) adopting the product due to peer pressure,

and terminate their use of the product either by

(c) stopping usage temporarily with a chance of re-adoption, or by

(d) stopping usage permanently.

S3.1 Model description

For a static social network G of size N and characterized by the adjacency matrix $\mathbf{A} = \{a_{ij}\}$, the probability $p_i^+(t)$ that individual i becomes a user at time t is given by,

$$p_i^+(t) = p_a + p_p(1 - p_a)n_i(t), \qquad n_i(t) = \frac{N_i(t)}{k_i}, \tag{S7}$$

where $p_a \in [0, 1]$ is the probability of spontaneously adopting the product, $p_p \in [0, 1]$ is the probability to be affected by peer pressure, $N_i(t)$ is the number of neighbours of i that at time t have already adopted the product, and $k_i = \sum_j a_{ij}$ its degree. Since the density of product users in the neighbourhood of i is $n_i(t)$, the time-dependent probability of adopting the product due to peer pressure is $p_p(1 - p_a)n_i(t)$. A peer pressure effect depending on the fraction of adopter neighbours rather than on their total number is reminiscent of other models of social activity, such as Watts' threshold model on global cascades [2].

Furthermore, the probability $p_i^-(t)$ that individual i stops being a user at time t is,

$$p_i^-(t) = p_r + p_s(1 - p_r), \tag{S8}$$

where $p_r, p_s \in [0, 1]$ are the probabilities of halting usage either permanently or temporarily. Overall, agents can be classified into sets of susceptible (S), adopting (A) and removed (R) individuals, describing respectively people who may adopt the product later, are users already, and will never use it again. The flow $S \to A$ is regulated by p_a and p_p, $A \to R$ by p_r, and $A \to S$ by p_s.

In the thermodynamic limit $N \to \infty$, the process of adoption at the user level can be well characterized with a master equation formalism. We assume that all agents with the same degree are statistically equivalent, allowing us to group individuals and write rate equations for each degree class k [3]. We denote by $s_k(t)$, $a_k(t)$ and $r_k(t)$ the average probabilities that a randomly chosen agent with degree k is susceptible, adopter and removed, respectively. In the limit of large system size these probabilities are equal to the densities of susceptible, adopting and removed individuals in the degree class k, so that $s_k + a_k + r_k = 1 \;\forall\, t, k$.

Let us denote by ρ_k the degree distribution of the static social network G, that is, the probability that a randomly chosen agent has degree k. With it the average probability of an individual belonging to the sets S, A and R are correspondingly given by

$$s(t) = \sum_k \rho_k s_k(t), \qquad a(t) = \sum_k \rho_k a_k(t), \qquad r(t) = \sum_k \rho_k r_k(t), \tag{S9}$$

with the normalization condition $s + a + r = 1 \;\forall\, t$. Our task is to find rate equations for the probabilities s_k, a_k and r_k that correspond to the dynamics set by Eqs. (S7) and (S8), solve them and average over the distribution ρ_k to get the time dependence of the probabilities s, a and r in Eq. (S9), so as to describe the evolution of the account network at a global level.

Through a simple first-order moment closure method, the rate equation for a_k can be written as $da_k/dt = \langle p_i^+ \rangle s_k - \langle p_i^- \rangle a_k$. In other words, the average probability that an adopting agent with degree k becomes either removed or susceptible is $\langle p_i^- \rangle a_k = [p_r + p_s(1 - p_r)]a_k$, while the average probability that a susceptible individual in the degree class k adopts the product is $\langle p_i^+ \rangle s_k = [p_a + p_p(1 - p_a)n_a]s_k$, where $n_a(t) = \langle n_i(t) \rangle$ is the average probability that the neighbour of a susceptible agent has adopted already. This approximation ignores higher moments of the dynamical quantities s_k, a_k and r_k, as well as any correlations between them. In the presence of degree-degree correlations in G,

$$n_a = \sum_{k'} \frac{k' - 1}{k'} \rho_{k',k} a_{k'}, \tag{S10}$$

with $\rho_{k',k}$ the conditional probability that an edge departing from an agent with degree k arrives at an agent with degree k' [3]. We can write similar equations for s_k and r_k to arrive at the system,

$$\frac{da_k}{dt} = [p_a + p_p(1-p_a)n_a]s_k - [p_r + p_s(1-p_r)]a_k \tag{S11}$$

$$\frac{ds_k}{dt} = -[p_a + p_p(1-p_a)n_a]s_k + p_s(1-p_r)a_k \tag{S12}$$

$$\frac{dr_k}{dt} = p_r a_k \tag{S13}$$

that forms a system of non-linear ordinary differential equations determining the adoption dynamics at the degree class level.

S3.2 Uncorrelated random networks

In order to progress further we need to simplify Eqs. (S11)-(S13) by making additional assumptions about the average probability n_a. If the social network G is considered as an uncorrelated random network, the conditional probability $\rho_{k',k}$ does not depend on k any more and it takes the simple form $\rho_{k',k} = k'\rho_{k'}/\langle k\rangle$, where $\langle k\rangle = \sum_k k\rho_k$ is the average degree in G. By substituting it into Eq. (S10) we obtain,

$$n_a = \frac{1}{\langle k\rangle}\sum_k (k-1)\rho_k a_k. \tag{S14}$$

Since the sum in n_a goes through all values of k, Eqs. (S11)-(S13) for all degree classes will be identical apart from initial conditions. In our case it is relevant to consider $s_k^0 = 1$ and $a_k^0 = r_k^0 = 0\ \forall\, k$, which further simplifies the dynamics and gives $a_k = a\ \forall\, k$, that is, $n_a = a(\langle k\rangle - 1)/\langle k\rangle$.

Moreover, since ρ_k is not a function of t, we can take an average by using Eq. (S9) and write,

$$\frac{da}{dt} = [p_a + p_{pk}(1-p_a)a]s - [p_r + p_s(1-p_r)]a \tag{S15}$$

$$\frac{ds}{dt} = -[p_a + p_{pk}(1-p_a)a]s + p_s(1-p_r)a \tag{S16}$$

now a planar system of non-linear ordinary differential equations that describes the evolution of the account network at a global level, where we have redefined the peer-pressure influence as the effective probability,

$$p_{pk} = \frac{\langle k\rangle - 1}{\langle k\rangle}p_p. \tag{S17}$$

For large values of $\langle k\rangle$, the effect of the social network's degree is minimal and $p_{pk} \sim p_p$.

The non-linear system in Eqs. (S15)-(S16) can be approached qualitatively by a linear stability analysis. The 0-clines of the system (i.e. the curves at which da/dt and ds/dt are respectively zero) can be written as,

$$s_a = \frac{[p_r + p_s(1-p_r)]a}{p_a + p_{pk}(1-p_a)a}, \qquad s_s = \frac{p_s(1-p_r)a}{p_a + p_{pk}(1-p_a)a}, \tag{S18}$$

so that $s_a - s_s = p_r a/[p_a + p_{pk}(1-p_a)a]$, and for $p_r \neq 0$ the only fixed point of the dynamics is $(a^\infty, s^\infty) = (0,0)$. Fig. S2A shows the flow of the system (S15)-(S16) and the 0-clines according to Eq. (S18).

By denoting $da/dt = f_a(a,s)$ and $ds/dt = f_s(a,s)$, the dynamics near the fixed point is determined by the Jacobian matrix,

$$J(a,s) = \begin{pmatrix} df_a/da & df_a/ds \\ df_s/da & df_s/ds \end{pmatrix} = \begin{pmatrix} p_{pk}(1-p_a)s - p_r - p_s(1-p_r) & p_a + p_{pk}(1-p_a)a \\ -p_{pk}(1-p_a)s + p_s(1-p_r) & -p_a - p_{pk}(1-p_a)a \end{pmatrix}, \tag{S19}$$

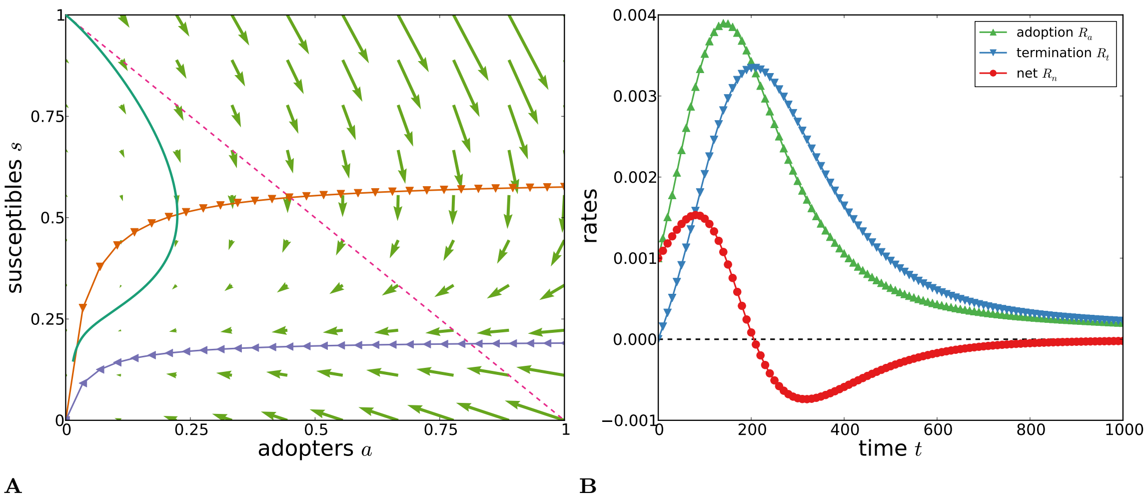

Figure S2. Numerical solution of the model process. (A) Phase portrait of the dynamics set by Eqs. (S15)-(S16). The arrows represent the flow of the dynamical system, symbols show the 0-clines s_a ($\triangledown$) and s_s ($\triangleleft$), and the dashed line is the upper limit for the allowed phase space (a, s) according to the condition $s + a + r = 1$. The continuous line is an example trajectory with initial condition $(a^0, s^0) = (0, 1)$ and parameters $p_a = 0.001$, $p_p = 0.05$, $p_s = 0.005$, $p_r = 0.01$ and $\langle k \rangle = 2$. (B) Time evolution of the rates of adoption (R_a), termination (R_t) and net change ($R_n = R_a - R_t$) for the same set of parameters.

i.e. $(da/dt, ds/dt) = J(0,0)(a,s)$ for $(a,s) \sim (0,0)$, and the stability of the fixed point is given by the eigenvalues $\lambda_\pm$ of $J(0,0)$,

$$0 = \begin{vmatrix} -p_r - p_s(1-p_r) - \lambda_\pm & p_a \\ p_s(1-p_r) & -p_a - \lambda_\pm \end{vmatrix} \implies \lambda_\pm = \frac{1}{2}\left(\tau \pm \sqrt{\tau^2 - 4\Delta}\right), \tag{S20}$$

where $\tau = -[p_a + p_r + p_s(1-p_r)] < 0$ and $\Delta = p_a p_r > 0$, as long as $p_a, p_r, p_s \neq 0$. Since $\tau < 0$ and $\tau^2 - 4\Delta > 0$ the fixed point is a stable node, meaning that (a^∞, s^∞) is indeed the final state of the dynamics and attracts all trajectories of the phase space. Fig. S2A shows an example trajectory starting from $(a^0, s^0) = (0, 1)$ for given parameter values, progressively approaching the fixed point.

Finally we consider the rates at which individuals adopt the product $[R_a(\mathrm{t})]$ and stop using it $[R_t(t)]$, as well as the rate of effective or net change $R_n(t) = R_a(t) - R_t(t)$, since they can be directly compared with the empirical data. By construction these are equal to the gain and loss terms in the rate equation for a, that is,

$$R_a(t) = [p_a + p_{pk}(1-p_a)a]s, \qquad R_t(t) = [p_r + p_s(1-p_r)]a. \tag{S21}$$

A numerical evaluation of the rates $R_a(t)$, $R_t(t)$ and $R_n(t)$ for given parameter values is shown in Fig. S2B.

S3.3 Numerical simulations

To verify our theoretical considerations we can implement the previous agent-based model and compare the solutions of Eq. (S21) with large-scale numerical simulations on synthetic network structures. The Skype network is strongly heterogeneous and presents a power-law like degree distribution as many other social networks. To get a similar structure for our numerical simulations we implement the Barabási-Albert model [3] and generate scale-free (SF) networks with a similar exponent, uncorrelated degrees and scalable average degree. We use this topology as a model for the background social network and on the top of it we perform the process defined by Eqs. (S7)-(S8).

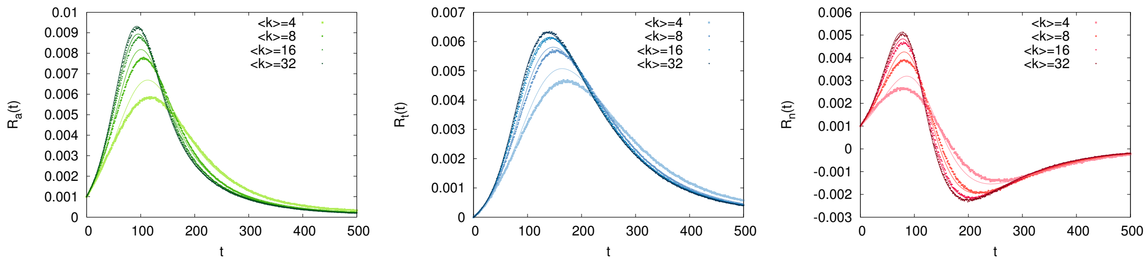

A $R_a(t)$ **B** $R_t(t)$ **C** $R_n(t)$

Figure S3. Numerical simulations of the adoption process on SF networks with different average degrees. We use networks with average degree $\langle k \rangle = 4$ (□), 8 (○), 16 (△), 32 (▽) and size $N = 10^5$. We show (A) the rate of adoption $R_a(t)$ (green), (B) the rate of termination $R_t(t)$ (blue), and (C) the rate of net change $R_n(t) = R_a(t) - R_t(t)$ (red). Symbols indicate averages of numerical simulations, while solid lines are curves derived from Eq. (S21) with parameters $p_a = 0.001$, $p_p = 0.05$, $p_s = 0.005$ and $p_r = 0.01$.

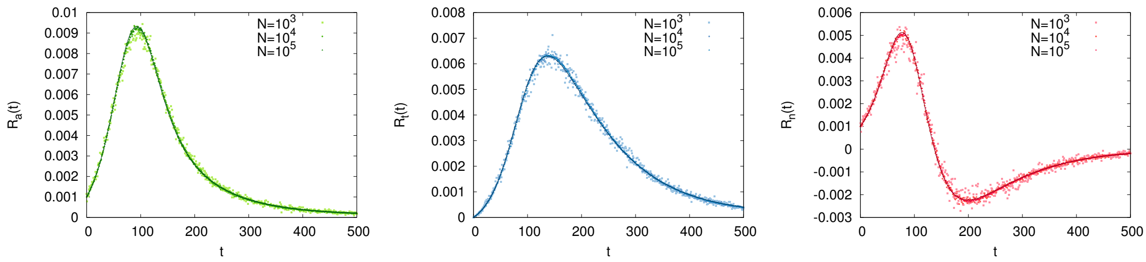

A $R_a(t)$ **B** $R_t(t)$ **C** $R_n(t)$

Figure S4. Numerical simulations of the adoption process on SF networks with different sizes. We use networks with size $N = 10^3$ (□), 10^4 (○), 10^5 (△) and average degree $\langle k \rangle = 32$. We show (A) the rate of adoption $R_a(t)$ (green), (B) the rate of termination $R_t(t)$ (blue), and (C) the rate of net change $R_n(t)$ (red). Symbols indicate averages of numerical simulations, while solid lines are curves derived from Eq. (S21) with the same parameter values as in Fig. S3.

During our theoretical considerations we have taken a mean-field approach that provides better accuracy if $N \to \infty$ and the average degree $\langle k \rangle$ of the background network is large. The validity of such approximation (and the correctness of our solution) can be verified by comparing the characteristic rates calculated from averages of large-scale simulations to the rates provided by Eq. (S21), while using the same parameter values. In Fig. S3 we show numerical simulations for synthetic networks with different average degrees, averaged over 100 realizations of the adoption process. As $\langle k \rangle$ increases the discrepancy between the theoretical and simulated rates reduces considerably, until finally in the limit of large $\langle k \rangle$ the fit between both rates is very accurate, validating our theoretical solution of the model.

The solution given in Eq. (S21) suggests no system size dependence of the normalized characteristic rates. This can be confirmed by simulations where only the size N of the static network is varied. The averages of 100 realizations shown in Fig. S4 indicate that even if in smaller networks the simulated rates have larger deviation, their averages overlap with the theoretical curve.

S3.4 Spreading scenarios

A careful selection of parameter values allows us to simulate various spreading scenarios. Simply by setting $p_r = 0$ we can reduce our model into a SIS-like dynamics [3] where a non-trivial equilibrium state appears. This is shown in Fig. S5A, where the system always ends up in a state with equal adoption and termination rates. It is also reflected by the cumulative sum giving the number of active nodes

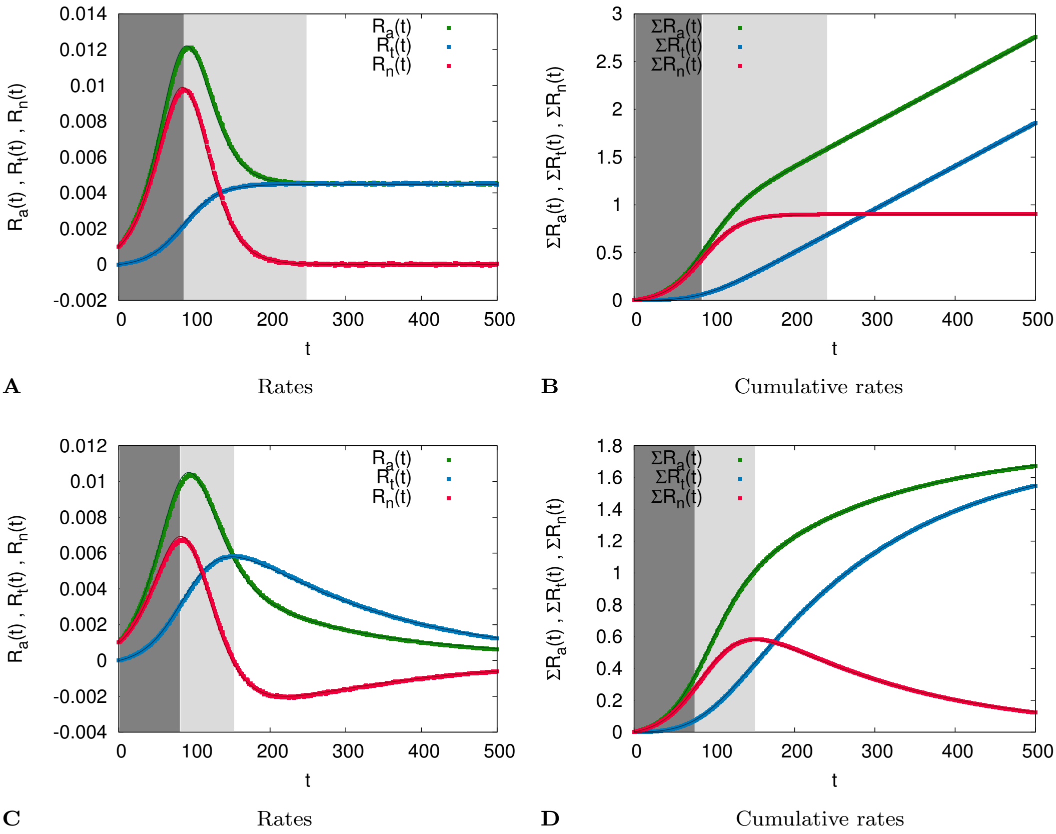

Figure S5. Numerical simulations and theoretical prediction of adoption processes. Processes were run with parameters $p_a = 0.001$, $p_p = 0.05$, $p_s = 0.005$ and $N = 10^5$, respectively for $p_r = 0$ (top) and $p_r = 0.005$ (bottom). Simulations are averaged over 100 realizations. On the left panels we show the rate of adoption $R_a(t)$ (green), the rate of termination $R_t(t)$ (blue) and the rate of net change $R_n(t) = R_a(t) - R_t(t)$ (red). On the right panels the corresponding cumulative functions are presented. Solid lines denote the associated theoretical curves. Shaded regions depict different regimes bounded by the characteristic times $\tau_0 = 0$, $\tau = \max(R_n(t))$ and $\tau_2 = R_n(t = 0^+)$, as well as $\tau_3 \to \infty$ (top) and $\tau_3 = R_n(t = 0^-)$ (bottom).

(red curve in Fig. S5B), which remains constant in the equilibrium state. The number of active users in equilibrium depends on the relative values of the adoption and termination probabilities. The evolution of the adoption process can be separated into three distinct regimes: In the initial regime from time $\tau_0 = 0$ until $\tau = \max(R_n(t))$ (dark-shaded region), the adoption spreads with an increasing speed and reaches the largest possible number of users. In the second regime from τ until $\tau_2 = R_n(t = 0^+)$ (light-shaded regime), the adoption spreading slows down as it becomes controlled by an increasing termination rate. In the third regime from τ_2 until $\tau_3 \to \infty$ (white region) the systems stays in equilibrium, which means no change in the account network size since the same number of users adopt and terminate in each time step.

A different scenario takes place if we allow agents to enter a removed state (see Fig. S5C). In this case the spreading process always reaches a trivial final state where no susceptible nodes remain and no more adoption can happen in the network. Its evolution can also be divided in three typical regimes, of which the first two are similar to the previous scenario. However, as in here termination to a removed state is also possible, the third regime spanning from τ_2 until $\tau_3 = R_n(t = 0^-)$ (white region) starts at a crossover point when termination becomes dominant, the adoption network starts to reduce and approaches the trivial final state. The same scenario can be followed in Fig. S5D where τ and τ_2 correspond respectively to the first inflection point and to the maximum of the curve measuring the total number of active users (red line).

S3.5 Non-trivial equilibrium states

The planar system in Eqs. (S15)-(S16) has a single fixed point $(0, 0)$ for nonzero p_r, meaning that the dynamics always ends up in a state where all individuals are removed and will never use the product again. A different spreading scenario can be obtained by setting $p_r = 0$, which leads to a non-trivial equilibrium state where the rates of adoption and termination are different from zero. Indeed, for $r = 0$ and $a + s = 1 \;\forall\, t$ the 0-clines of Eq. (S18) become equal,

$$s_a = s_s = \frac{p_s a}{p_a + p_{pk}(1 - p_a)a}, \tag{S22}$$

and the final state (a^∞, s^∞) can be found by inserting Eq. (S22) in the normalization condition $s^\infty = 1 - a^\infty$. The resulting quadratic equation gives,

$$a^\infty_\pm = \frac{1}{2p_{pk}(1 - p_a)} \left[p_{pk}(1 - pa) - p_a - p_s \pm \sqrt{[p_{pk}(1 - p_a) - p_a - p_s]^2 + 4p_a p_{pk}(1 - p_a)} \right]. \tag{S23}$$

Since $4p_a p_{pk}(1 - p_a) > 0$ for $p_a, p_{pk} \neq 0$, we have $a^\infty_- < 0$ and the stationary probability of adoption can only be $a^\infty = a^\infty_+ \neq 0$. Moreover, the condition $da/dt = 0$ defining the final state implies that the stationary rates of adoption and termination are equal to an equilibrium rate $R^\infty = p_s a^\infty$, which after some algebra can be written as,

$$R^\infty = \frac{p_s}{2} \left(1 - \frac{p_a + p_s}{p_{pk}(1 - p_a)} + \sqrt{\left[1 - \frac{p_a + p_s}{p_{pk}(1 - p_a)} \right]^2 + \frac{4p_a}{p_{pk}(1 - p_a)}} \right). \tag{S24}$$

The condition $p_r = 0$ simplifies the system (S15)-(S16) into the single autonomous equation $da/dt = [p_a + p_{pk}(1 - p_a)a](1 - a) - p_s a$. After integrating directly and rearranging terms with the help of Eq. (S23) we obtain,

$$a(t) = a^\infty_+ \frac{e^{t/\tau_c} - 1}{e^{t/\tau_c} - a^\infty_+ / a^\infty_-}, \tag{S25}$$

where we have defined a characteristic time $\tau_c = 1/\sqrt{[p_{pk}(1 - p_a) - p_a - p_s]^2 + 4p_a p_{pk}(1 - p_a)}$. The explicit solution in Eq. (S25) can be used to derive analytical expressions for the temporal evolution of the rates R_a and R_t of Eq. (S21), which in turn lead to expressions of important moments in the dynamics like the times t_a and t_n, defined respectively as the times when the rates R_a and $R_n = R_a - R_t$ are maximal. Explicitly,

$$t_a = \tau_c \ln \left(\frac{a^\infty_+}{a^\infty_-} \cdot \frac{-p_s - 1/\tau_c}{-p_s + 1/\tau_c} \right) \qquad \text{and} \qquad t_n = \tau_c \ln \left(- \frac{p_{pk}(1 - p_a) - p_a - p_s + 1/\tau_c}{p_{pk}(1 - p_a) - p_a - p_s - 1/\tau_c} \right). \tag{S26}$$

Since da/dt is autonomous, we can also find the maximal rates of adoption and net change ($R^*_a = R_a(t_a)$ and $R^*_n = R_n(t_n)$) through a quicker route. The condition $0 = dR_a/dt|_{t=t_a}$ implies $2a(t_a) = 1 - p_a/[p_{pk}(1 - p_a)]$, so we can substitute in the left side of Eq. (S21) and write,

$$R^*_a = \frac{p_a}{4} \left(1 + \frac{p_a}{p_{pk}(1 - p_a)} \right) \left(1 + \frac{p_{pk}(1 - p_a)}{p_a} \right). \tag{S27}$$

Similarly, for the net rate we have $2a(t_n) = 1 - (p_a + p_s)/[p_{pk}(1 - p_a)]$ and,

$$R^*_n = \frac{1}{4} \left(1 + \frac{p_a + p_s}{p_{pk}(1 - p_a)} \right) [p_a + p_{pk}(1 - p_a) - p_s] - \frac{p_s}{2} \left(1 - \frac{p_a + p_s}{p_{pk}(1 - p_a)} \right). \tag{S28}$$

Eqs. (S24), (S27) and (S28) define a non-linear algebraic system between the rates $\{R^\infty, R^*_a, R^*_n\}$ and the parameters $\{p_a, p_{pk}, p_s\}$, one that may be used to solve the inverse problem of determining appropriate parameters in terms of measured rates. The resulting parameters and their errors give in this way estimated areas for the time evolution of the rates in the system.

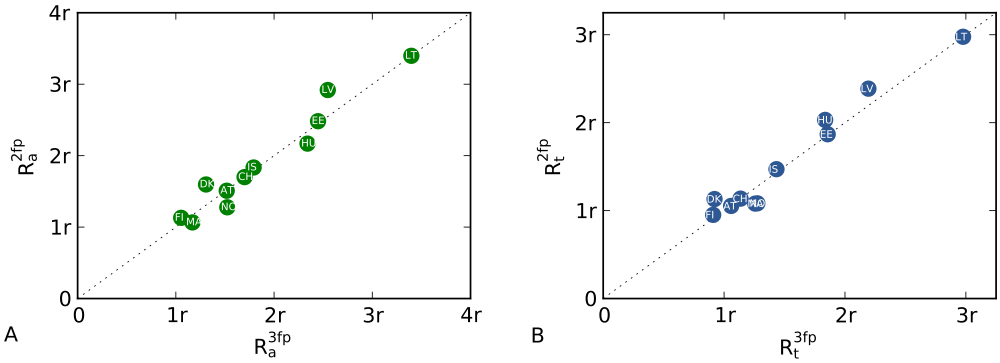

Figure S6. Comparison between model predictions. Predictions obtained by fits with three (x-axis) and two (y-axis) free parameters are shown for the 11 different countries where $\widetilde{p_a}$ is empirically determinable. Symbols depict (a) rates of adoption $R_a(t)$ (green) and (b) rates of termination $R_t(t)$ (blue) averaged over the last six months of the observation period, with their corresponding standard deviations as error bars (smaller than symbols). In-symbol letters are country abbreviations, r is an arbitrary linear scaling constant, and the dashed line is a linear function with unit slope.

S4 Empirical fits

To obtain the best model fit of the empirical rates we apply a bounded non-linear least square method and fit the binned $R_a(t)$, $R_t(t)$, and $R_n(t)$ curves simultaneously. As discussed in the main text, the model is determined by the parameter set $\{p_a, p_p, p_r, \widetilde{p_s}, \widetilde{\langle k \rangle}\}$. There we present fitting results where $\{\widetilde{p_s}, \widetilde{\langle k \rangle}\}$ are always estimated from the data and $\{p_a, p_p, p_r\}$ are considered as free parameters. However, in some countries the data allows for the empirical determination of $\widetilde{p_a}$ as well. Out of the 34 investigated countries, we could estimate this parameter empirically for 11 countries and perform the fitting with the parameter set $\{\widetilde{p_a}, p_p, p_r, \widetilde{p_s}, \widetilde{\langle k \rangle}\}$ of two free (p_p, p_r) and three fixed $(\widetilde{p_a}, \widetilde{p_s}, \widetilde{\langle k \rangle})$ parameters.

S4.1 Two vs. three free parameter fits

In Fig. S6 we compare the predicted modelled rates obtained by fitting the empirical rates with either two or three free parameters. Although some differences appear between the two results, in most countries the corresponding symbols collapse in a line with unit slope and thus assign excellent agreement between the predicted rates. This implies that even fits with three free parameters provide good predictions about the asymptotic evolution of the adoption process.

S4.2 Goodness of fits

To quantify the quality of the obtained empirical fits we performed the following analysis. The model fit is calculated over the first 5 years of the data, so that the end of the training period is always fixed. In contrast the beginning of the training period may slightly vary from country to country, depending on the length of the initial transient state. Consequently, a comparable fit quality measure is calculated as follows: The model rates are fitted over the curves r_a^e, r_t^e and r_n^e, each a group of 10 (or less) binned empirical values of $R_a(t)$, $R_t(t)$ and $R_n(t)$, respectively. We then derive the triplet,

$$r_* = \left(\frac{r_*^e - \overline{r_*^m}}{\max(r_*^e)} \right)^2, \tag{S29}$$

where $* \in \{a, t, n\}$ and $\overline{r_*^m}$ is the corresponding average model value. Using this triplet we calculate the combined Residual Sum of Squares (RSS) per point set as,

$$RSS = \frac{\sum_{t=n_{min}}^{n} r_a(t) + r_t(t) + r_n(t)}{n - n_{min}}, \tag{S30}$$

where n is an index of measure points ($\max(n) = 10$) and n_{min} is the minimum index of the actual country measure. The obtained RSS values are summarized in Table S1.

Abbreviation	Country name	RSS (3 free parameters)	RSS (2 free parameters)
AT	Austria	0.030547	0.030640
CH	Switzerland	0.089469	0.089468
DK	Denmark	0.089758	0.111208
EE	Estonia	0.083691	0.084199
FI	Finland	0.094170	0.336367
HU	Hungary	0.075269	0.378541
IS	Iceland	0.091920	0.045883
LV	Latvia	0.021787	0.045755
LT	Lithuania	0.130222	0.130222
MA	Morocco	0.178242	1.058968
NO	Norway	0.065166	0.048559

Table S1. List of investigated countries with three or two free parameters fits. The first and second columns give the country abbreviation codes and names, while the third and forth column includes the corresponding combined RSS values (defined in section S4) obtained by three and two free parameter fits respectively.

S4.3 Correlations with liberty measures

As mentioned in the main text, our model of adoption spreading can disclose relevant differences between the adoption dynamics of countries at various levels of societal and economical development. One characteristic indicator in focus is the average lifetime of accounts in a given country defined as $\langle t_l \rangle = \langle t_t - t_a \rangle$, where t_a and t_t are the corresponding registration and termination times. We relate this empirical measure to general liberty measures [4] with results shown in the main text and in Fig.S7. We observe that the weaker the press/political/civil liberty is in a country, the shorter time online accounts are used there. Such observations indicate a quantifiable dependence between the dynamics of innovation spreading and the socio-economic status of a country.

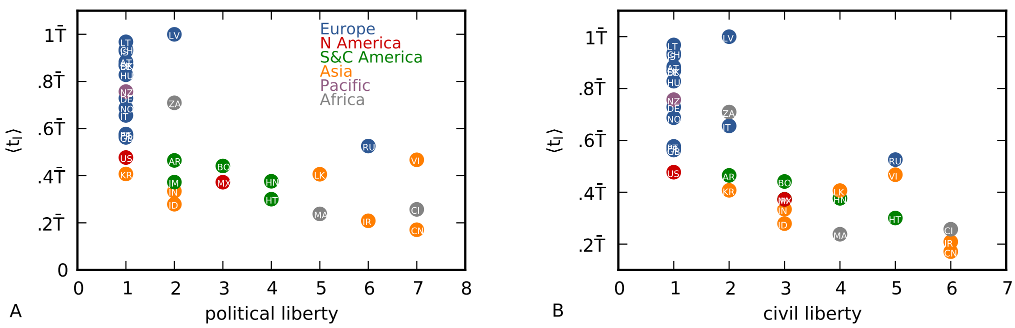

Figure S7. Account life time correlations with liberty measures. Average lifetime $\langle t_l \rangle$ of accounts as a function of (a) political and (b) civil liberty measures [4] in various countries (large scores imply weak liberties). $\bar{T}$ is an arbitrary linear scaling constants with time dimension.

References and notes

[1] Morrissey RC, Goldman ND, Kennedy KP. 2011 Skype S.A. United States Security Registration Statement, Amendment 3, Reg.No. 333-168646 (Date of access: 15/06/2013).

[2] Watts DJ. 2002 A simple model of global cascades on random networks. *Proc. Natl. Acad. Sci. USA* **99**, 5766–5771. (DOI 10.1073/pnas.082090499.)

[3] Barrat A, Barthelemy M, Vespignani A. 2008 *Dynamical Processes on Complex Networks* (Cambridge Univ. Press, Cambridge).

[4] Freedom in the World.2011 *www.freedomhouse.org* (Date of access: 06/03/2013).